SUPPLEMENTAL DATA

EXPERIMENTAL PROCEDURES

Deconvolution of protein secondary structure by FTIR spectroscopy - Amide I components corresponding to the side chains, i.e. those within 1615-1600 cm^{-1} for the unlabeled protein and 1565-1550 cm^{-1} for the ^{13}C-labeled protein, were subtracted, and the sum of the areas of all remaining components was used as the total amide I area (A_T). The components that correspond to α-helix, β-sheet, and irregular structure were identified following standard assignment procedures (*1-5*), as shown in Table S1. For the ^{13}C-labeled protein, all amide I components were considered to be downshifted by 45-50 cm^{-1}, as shown earlier (6,7). The antiparallel β-sheet has two components, one around 1635 cm^{-1} and the other in the 1680-1670 cm^{-1} region, and the extinction coefficient of the latter constitutes 7% of the former (*8*). Therefore, the total β-sheet fraction was determined by multiplying the fraction of the low frequency β-sheet component area ($A_{\beta,low}$) by 1.07. The sum of the components between 1700-1660 cm^{-1} (1650-1610 cm^{-1} for the ^{13}C-labeled protein), minus $0.07\times A_{\beta,low}$, was assigned to various types of turn structures. According to the Beer-Lambert law:

$$A_T = \sum l\varepsilon_i C_i \tag{1}$$

where l is the optical path-length, ε_i and C_i are the extinction coefficients and the concentrations of the ith structural component, side chains excluded. From Eq. (1) we obtain the following expression for the concentration of ith secondary structure:

$$C_i = \frac{A_T - \sum_{j\neq i} l\varepsilon_j C_j}{l\varepsilon_i} \tag{2}$$

The numerator in Eq. (2) is simply the area of the ith component, a_i, therefore it can be re-written as follows:

$$C_i = \frac{a_i}{l\varepsilon_i} \tag{3}$$

The fraction of the ith secondary structure in the protein is:

$$f_i = \frac{C_i}{C} \tag{4}$$

where C is the total concentration of all secondary structural elements and is given as follows:

$$C = \sum \frac{a_i}{l\varepsilon_i} \tag{5}$$

In Eq. (5), the summation is over all secondary structures. This approach requires the amide I areas and the extinction coefficients of all secondary structures. The extinction coefficients of α-helix, β-sheet, and irregular structure have been experimentally determined (*8*), but those of various types of turns and other structures are not known. A reasonable approach is to consider the protein as consisting of four types of secondary structure, i.e., α-helix, β-sheet, irregular (ρ) structure, and "other", primarily including turns and other structures. For the "other", an extinction coefficient can be used that is the average of those of α-helix, β-sheet (the low frequency counterpart), and ρ-structure. With this, Eq. (5) can be re-written as follows:

$$C = \frac{a_\alpha}{l\varepsilon_\alpha} + \frac{a_\beta}{l\varepsilon_\beta} + \frac{a_\rho}{l\varepsilon_\rho} + \frac{a_{other}}{l\varepsilon_{other}} \tag{6}$$

Equations (3), (4) and (6) yield:

$$f_i = \frac{a_i}{\varepsilon_i\left(\frac{a_\alpha}{\varepsilon_\alpha} + \frac{a_\beta}{\varepsilon_\beta} + \frac{a_\rho}{\varepsilon_\rho} + \frac{a_{other}}{\varepsilon_{other}}\right)} \tag{7}$$

For extinction coefficients of the α-helix, β-sheet, ρ-structure and the "other" structures in D_2O-based buffers, the following values have been used: $\varepsilon_\alpha = 5.1\times10^7$ cm/mol, $\varepsilon_\beta = 7.0\times10^7$ cm/mol, $\varepsilon_\rho = 4.5\times10^7$ cm/mol, $\varepsilon_{other} = 5.5\times10^7$ cm/mol (*8*). These are the "integrated" extinction coefficients, based on the band area rather than height, which is more appropriate within the current approach.

In case of spectra of two proteins combined in one sample, one unlabeled (i.e., ^{12}C) and other ^{13}C-labeled, the amide I components belonging to each protein were identified. Together with respective extinction coefficients, eight fractions were identified: $f_{\alpha,12C}$, $f_{\beta,12C}$, $f_{\rho,12C}$, $f_{other,12C}$, $f_{\alpha,13C}$, $f_{\beta,13C}$, $f_{\rho,13C}$, and $f_{other,13C}$ using Eq. (7), and were corrected as follows. Each of the eight fractions was multiplied by the total number of amino acid residues in two proteins and then divided by the number of amino acid residues in the respective (i.e., ^{12}C or ^{13}C) protein to determine the protein secondary structure.

The criteria we used were not only the "goodness of fit" (i.e., the match between the measured spectrum and the "curvefit"), but also the correspondence between the frequencies of the components to those predicted by the second derivative spectra. Our assignments of amide I components to certain secondary structures are based on established standards (*1-5*). We are aware that some secondary structures may generate amide frequencies at slightly different wavenumbers (i.e., "fingerprint frequencies" - (*2*)). Therefore, consistent with published guidelines, our assignments used a certain range rather that a fixed wavenumber for each secondary structure (Table S1). Still, there are components that cannot be assigned to certain structural elements with a high degree of confidence. Therefore, our assignments include a component termed "other" which can include various types of turns and other structures that are different from α-helix or β-sheet.

In our data analysis, we did not adhere to an assumption that all components were shifted by exactly 50 cm^{-1}. Instead, the curve-fitting of each amide I spectrum was based on its own second derivative. Assignment of the amide I components of ^{13}C-labeled protein was conducted using such assignment of the unlabeled protein as a guideline, keeping in mind that the ^{13}C-labeling will cause approximately 45-50 cm^{-1} downshift.

CD - Measurements were taken in a 4 mm path length cuvette using a Jasco 810 spectrofluoropolarimeter with a PFD-425S Peltier temperature controller. Protein concentration was 73 μg in 220 μl of 10 mM sodium borate buffer (pH 7.0) containing 100 mM NaCl. Measurements were recorded at 10°C, 20°C, 30°C, 37°C, and 45°C after incubating the sample for 10 min at each temperature.

Protease sensitivity assay - 8 μg of a purified CTA1-CTA2 heterodimer was added to 160 μl of 20 mM sodium phosphate buffer (pH 7.0) containing 10 mM β-mercaptoethanol in the presence or absence of an equimolar concentration of PDI. Toxin aliquots of 20 μl were incubated at the indicated times for 1 h. All samples were then placed on ice for 10 min. Thermolysin was then added to a final concentration of 0.04 mg/ml, and the samples were incubated at 4°C for 1 hr. Digests were stopped with the addition of 10 mM ethylenediaminetetraacetic acid, and the toxin samples were visualized by SDS-PAGE with Coomassie staining.

SUPPLEMENTAL REFERENCES

1. Jackson, M., and Mantsch, H. H. (1995) *Crit Rev Biochem Mol Biol* **30,** 95-120
2. Tatulian, S. A. (2003) *Biochemistry* **42,** 11898-11907
3. Tatulian, S. A., Cortes, D. M., and Perozo, E. (1998) *FEBS Lett* **423,** 205-212
4. Kong, J., and Yu, S. (2007) *Acta Biochim Biophys Sin (Shanghai)* **39,** 549-559
5. Haris, P. I. (2010) *Biochem Soc Trans* **38,** 940-946
6. Tatulian, S. A., Chen, B., Li, J., Negash, S., Middaugh, C. R., Bigelow, D. J., and Squier, T. C. (2002) *Biochemistry* **41,** 741-751
7. Tatulian, S. A., Qin, S., Pande, A. H., and He, X. (2005) *J Mol Biol* **351,** 939-947
8. Venyaminov, S., and Kalnin, N. N. (1990) *Biopolymers* **30,** 1259-1271
9. O'Neal, C. J., Jobling, M. G., Holmes, R. K., and Hol, W. G. (2005) *Science* **309,** 1093-1096
10. Zhang, R. G., Scott, D. L., Westbrook, M. L., Nance, S., Spangler, B. D., Shipley, G. G., and Westbrook, E. M. (1995) *J Mol Biol* **251,** 563-573

Wavenumbers (cm^{-1})	Assignment
1604 ± 4	α-helix
1577 ± 7	β-sheet
1593 ± 5	irregular

TABLE S1. **Deconvoluted amide I band frequencies and assignments to secondary structure for ^{13}C-labeled CTA1 in $D_2$0.**

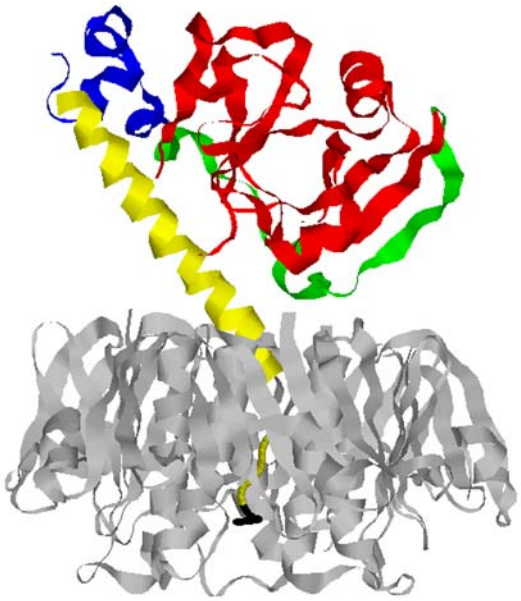

FIGURE S1. **Ribbon diagram of CT.** The presented CT structure is based upon data reported by O'Neal et al. (PDB 1S5F) (*9*), and the partitioning of CTA1 into subdomains is based upon data reported by Zhang et al. (*10*). The $CTA1_1$ subdomain is shown in red; the $CTA1_2$ subdomain is presented in green; and the $CTA1_3$ subdomain is shown in blue. CTA2 is presented in yellow, with the C-terminal KDEL tag shown in black. The CTB pentamer is grey.

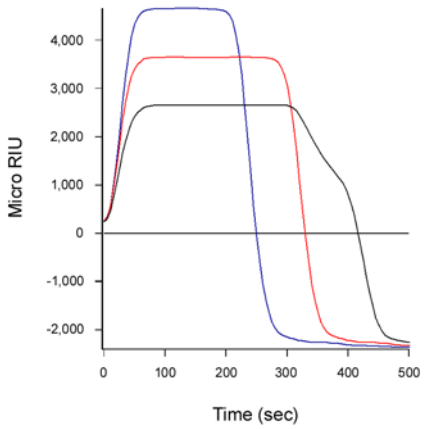

FIGURE S2. **Concentration-dependent kinetics of CT disassembly by PDI.** After appending CT to a GM1-coated SPR sensor slide, a baseline measurement corresponding to the mass of the CT holotoxin was recorded. Reduced PDI (PDI + 1 mM GSH) was then perfused over the CT sensor slide at concentrations of 100 μM (blue line), 10 μM (red line), or 1 μM (black line). PDI was present in the perfusion buffer throughout the experiment.

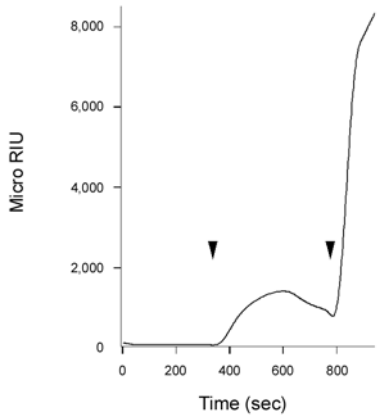

FIGURE S3. **Lack of PDI interaction with CTA2/CTB$_5$.** CTA2/CTB$_5$ was appended to a GM1-coated SPR sensor slide. Reduced PDI (PDI + 1 mM GSH) was then perfused over the CTA2/CTB$_5$ sensor slide for 380 sec. Sequential additions of anti-KDEL and anti-CTB antibodies, denoted by the arrowheads, were used as positive controls.

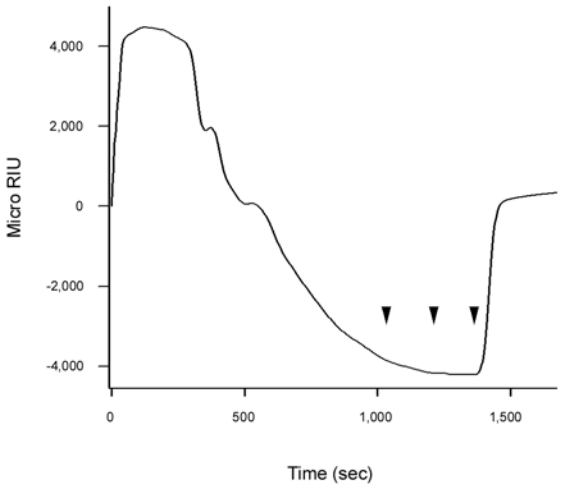

FIGURE S4. **CT disassembly at 4°C.** After appending CT to a GM1-coated sensor slide, a baseline measurement corresponding to the mass of the bound holotoxin was recorded. Reduced PDI (PDI + 1 mM GSH) was then perfused over the CT-coated sensor at 4°C. PDI was removed 1,000 sec into the experiment and replaced with sequential additions of anti-PDI, anti-CTA, and anti-KDEL antibodies as indicated by the arrowheads.

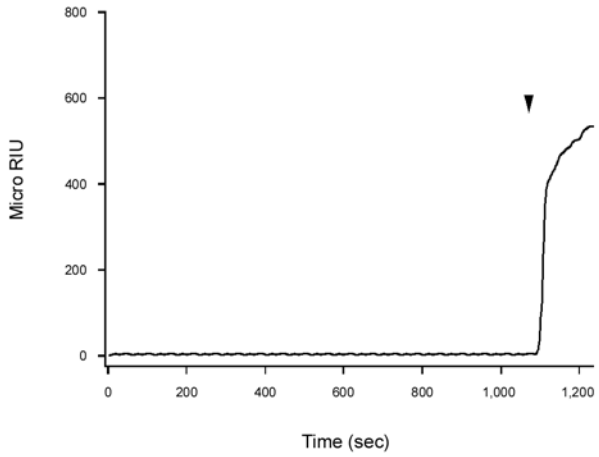

FIGURE S5. **The reduced CT holotoxin remains intact after thermal denaturation of CTA1.** CT was appended to a GM1-coated SPR sensor slide, and a baseline measurement corresponding to the mass of the bound holotoxin was recorded. The CT-coated sensor slide was then heated to 65°C in perfusion buffer containing 1 mM GSH. After 1,000 sec at 65°C, the slide was cooled to 37°C and exposed to perfusion buffer containing an anti-CTA antibody as marked by the arrowhead.

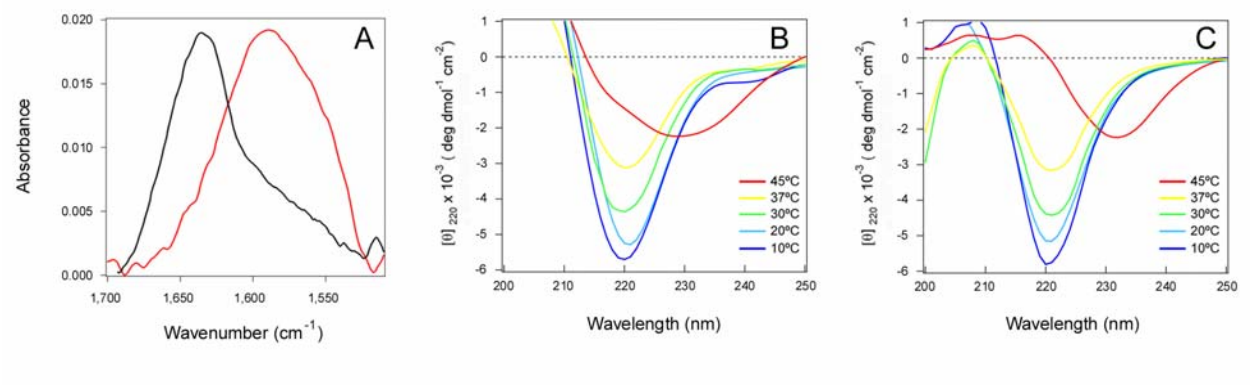

FIGURE S6. **Effect of ^{13}C-labeling on the FTIR and circular dichroism spectra of CTA1.** (A): FTIR spectra of CTA1 (black line) and ^{13}C-labeled CTA1 (red line) were recorded at 37°C. (B-C): Far-UV circular dichroism spectra of ^{13}C-labeled CTA1 (B) or unlabeled CTA1 (C) were recorded at the indicated temperatures.

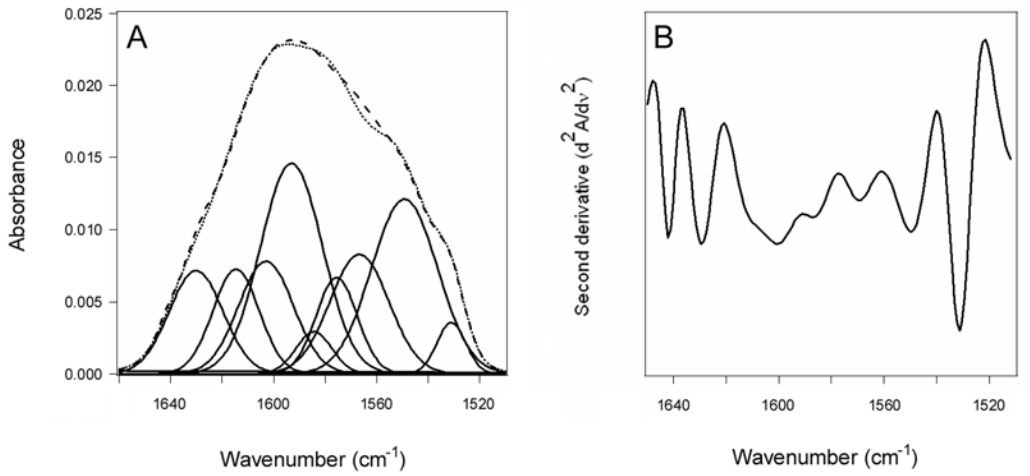

FIGURE S7. **The 37°C structure of CTA1.** Curve-fitting (A) and second derivative (B) for the FTIR spectrum of ^{13}C-labeled CTA1 are shown. In panel A, the dotted line represents the sum of all deconvoluted components (solid lines) from the measured spectrum (dashed line).

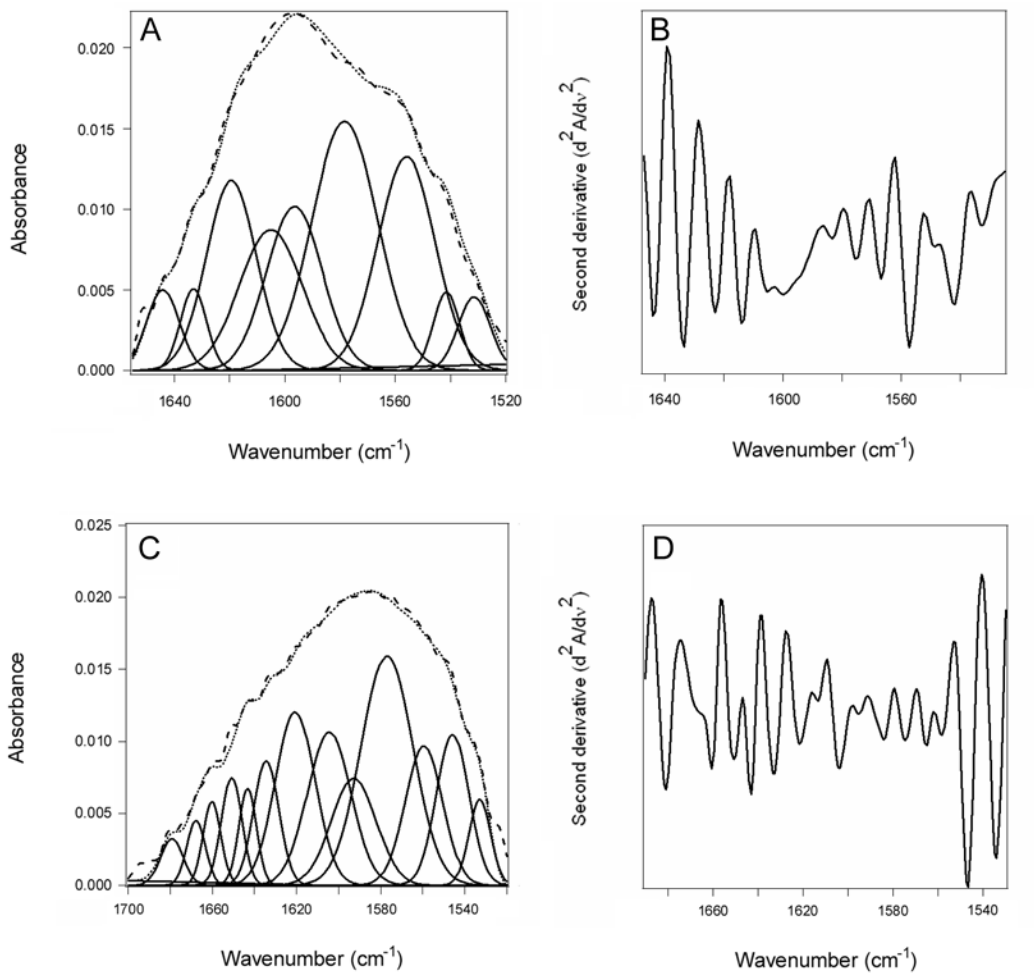

FIGURE S8. **The 30°C structure of CTA1 in the absence or presence of PDI.** Curve-fitting (A, C) and second derivatives (B, D) for the FTIR spectrum of ^{13}C-labeled CTA1 recorded in the absence (A, B) or presence (C, D) of PDI are shown. In panels A and C, the dotted line represents the sum of all deconvoluted components (solid lines) from the measured spectrum (dashed line). Note that different wavenumber scales are used in panels A and B than in panels and C and D.

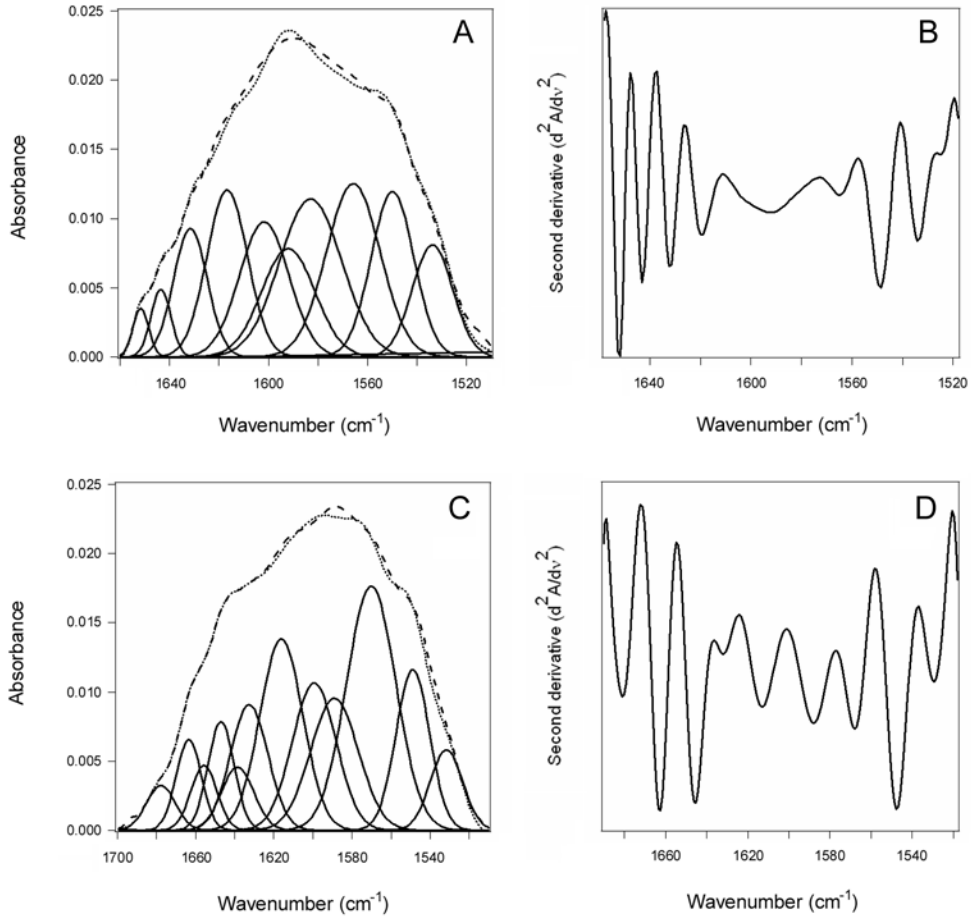

FIGURE S9. **The 37°C pH 6.5 structure of CTA1 in the absence or presence of PDI.** Curve-fitting (A, C) and second derivatives (B, D) for the FTIR spectrum of ^{13}C-labeled CTA1 recorded in the absence (A, B) or presence (C, D) of PDI are shown. In panels A and C, the dotted line represents the sum of all deconvoluted components (solid lines) from the measured spectrum (dashed line). Note that different wavenumber scales are used in panels A and B than in panels and C and D.

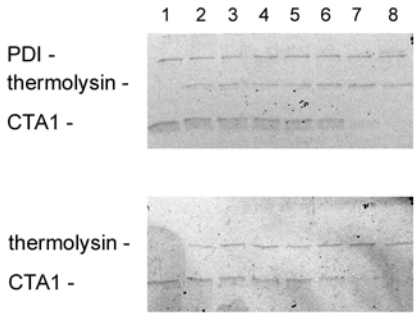

FIGURE S10. **Temperature- and PDI-induced shift of CTA1 to a protease-sensitive conformation.** The reduced CTA1/CTA2 heterodimer was incubated in the presence (top panel) or absence (bottom panel) of PDI for 1 h at 4°C (lanes 1 and 2), 10°C (lane 3), 20°C (lane 4), 25°C (lane 5), 30°C (lane 6), 37°C (lane 7), or 40 (lane 8). All samples except lane 1 were then exposed to the protease thermolysin for 1 h at 4°C. Samples were visualized with SDS-PAGE and Coomassie staining, which does not detect the 5 kDa CTA2 subunit.